Published in final edited form as:
J Med Genet. 2013 August ; 50(8): 543–551. doi:10.1136/jmedgenet-2013-101542.

A *de novo* X;8 translocation creates a *PTK2-THOC2* gene fusion with *THOC2* expression knockdown in a patient with psychomotor retardation and congenital cerebellar hypoplasia

Eleonora Di Gregorio[1,2], **Federico T. Bianchi**[3], **Alfonso Schiavi**[4,5], **Alessandra M.A. Chiotto**[3], **Marco Rolando**[6], **Ludovica Verdun di Cantogno**[7], **Enrico Grosso**[2], **Simona Cavalieri**[2], **Alessandro Calcia**[1], **Daniela Lacerenza**[1], **Orsetta Zuffardi**[8,9], **Saverio Francesco Retta**[10], **Giovanni Stevanin**[11,12], **Cecilia Marelli**[11,12], **Alexandra Durr**[11,12], **Sylvie Forlani**[11], **Jamel Chelly**[13], **Francesca Montarolo**[14], **Filippo Tempia**[14], **Hilary E. Beggs**[15], **Robin Reed**[16], **Stefania Squadrone**[17], **Maria C. Abete**[17], **Alessandro Brussino**[1], **Natascia Ventura**[4,5], **Ferdinando Di Cunto**[3], and **Alfredo Brusco**[1,2,*]

[1]University of Torino, Department of Medical Sciences, Italy

[2]S.C.d.U. Medical Genetics, Città della Salute e della Scienza, Torino, Italy

[3]University of Torino, Department of Molecular Biotechnology and Health Sciences, Molecular Biotechnology Centre, Via Nizza 52, 10126, Torino, Italy

[4]University of Roma “Tor Vergata”, Department of Biomedicine and Prevention, Italy

[5]Institute of Clinical Chemistry and Laboratory Medicine of the Heinrich Heine University, and the IUF - Leibniz Research Institute for Environmental Medicine, Duesseldorf, Germany

[6]S.C. Neuropsichiatria Infantile, ASL TO3, Pinerolo, Italy

[7]S.C.d.U. Anatomia Patologica, Città della Salute e della Scienza, Torino, Italy

[8]Department of Molecular Medicine, University of Pavia, Pavia, Italy

[9]IRCCS “National Neurological Institute C. Mondino” Foundation, Pavia, Italy

[10]Department of Clinical and Biological Sciences, University of Turin, Orbassano, Italy

[11]Centre de Recherche de l’Institut du Cerveau et de la Moelle épinière (INSERM/UPMC Univ. Paris 6, UMR_S975; CNRS 7225, EPHE), Pitié-Salpêtrière Hospital, Paris, France

[12]APHP, Fédération de génétique, Pitié-Salpêtrière Hospital, Paris, France

[13]Université Paris Descartes, Institut Cochin - Hôpital Cochin, Paris - France

[14]University of Torino, Neuroscience Institute Cavalieri Ottolenghi (NICO), Torino, Italy

[15]Department of Ophthalmology, University of California San Francisco, San Francisco, CA 94122, USA

[*]Corresponding author: Alfredo Brusco, Department of Medical Sciences University of Torino, via Santena, 19 - 10126 Torino, Italy. Fax: +39 011 670 5668; alfredo.brusco@unito.it.

Conflict of interest: The authors declare no conflict of interest

[16]Department of Cell Biology, Harvard Medical School, Boston, USA

[17]Istituto Zooprofilattico Sperimentale del Piemonte, Liguria e Valle d'Aosta, CReAA- National Reference Centre for Surveillance and Monitoring of Animal Feed, Lab. Contaminanti Ambientali, Torino, Italy

Abstract

We identified a balanced *de novo* translocation involving chromosomes Xq25 and 8q24 in an eight year-old girl with a non-progressive form of congenital ataxia, cognitive impairment and cerebellar hypoplasia. Breakpoint definition showed that the promoter of the *Protein Tyrosine Kinase 2* (*PTK2*, also known as *Focal Adhesion Kinase, FAK*) gene on chromosome 8q24.3 is translocated 2 kb upstream of the THO complex subunit 2 (*THOC2*) gene on chromosome Xq25. *PTK2* is a well-known non-receptor tyrosine kinase whereas *THOC2* encodes a component of the evolutionarily conserved multiprotein THO complex, involved in mRNA export from nucleus. The translocation generated a sterile fusion transcript under the control of the *PTK2* promoter, affecting expression of both *PTK2* and *THOC2* genes. PTK2 is involved in cell adhesion and, in neurons, plays a role in axonal guidance, and neurite growth and attraction. However, *PTK2* haploinsufficiency alone is unlikely to be associated with human disease. Therefore, we studied the role of THOC2 in the CNS using three models: 1) *THOC2* ortholog knockout in *C. elegans* which produced functional defects in specific sensory neurons; 2) *Thoc2* knockdown in primary rat hippocampal neurons which increased neurite extension; 3) *Thoc2* knockdown in neuronal stem cells (LC1) which increased their in vitro growth rate without modifying apoptosis levels. We suggest that *THOC2* can play specific roles in neuronal cells and, possibly in combination with *PTK2* reduction, may affect normal neural network formation, leading to cognitive impairment and cerebellar congenital hypoplasia.

Keywords

chromosomal translocation; PTK2; FAK; THOC2; cerebellar hypoplasia

INTRODUCTION

Cerebellar malformations are rare developmental disorders that comprise many heterogeneous diseases, with both acquired and genetic causes [1]. They can be confined to the cerebellum or variably involve other infratentorial or supratentorial structures, such as the brainstem, the corpus callosum and the cerebral cortex [2]. The cerebellum is usually hypoplastic, at difference from neurodegenerative disorders, in which progressive cerebellar atrophy is observed.

Nevertheless, the distinction between cerebellar hypoplasia and cerebellar atrophy is not always clear-cut, as secondary atrophy may occur in a hypoplastic cerebellum. Both syndromic and pure forms of cerebellar hypoplasia are known. The clinical spectrum associated with cerebellar hypoplasia varies according to the aetiology, and includes non-progressive congenital ataxia (NPCA), abnormal ocular movements and, less frequently, hypotonia. Besides motor deficits, clinical features may include developmental delay,

cognitive impairment, deficit of executive functions, language deficits, and mood disorders including autistic-like behaviour [3]. The genetic component has been partially defined in recent years, and autosomal recessive, autosomal dominant or X-linked inheritance have been reported (http://neuromuscular.wustl.edu/ataxia/recatax.html#congenital). At least 15 syndromes with cerebellar hypoplasia have X-linked inheritance. For some of them causative genes have been identified (e.g. *OPHN1*, *DKC1*, *CASK* and *CUL4B)* [4, 5], while two additional loci have been mapped to Xp11.21-Xq24 [6, 7] and Xq25-q27.1 [8], respectively.

Here we report the detailed investigation, starting from the abnormal karyotype, in a child affected by cerebellar hypoplasia, non-progressive congenital ataxia, and psychomotor delay. Cytogenetic and breakpoint analyses led to the identification of genes potentially involved in the disease, a role corroborated by functional analyses.

MATERIALS AND METHODS

Subjects, cell lines, and extraction of genomic DNA and total RNA

Peripheral blood lymphocytes (PBL) were obtained from the patient and her parents. PBL were used to create immortalized lymphoblastoid cell lines (LCL) by Epstein-Barr Virus (EBV) transformation. Fibroblasts were obtained from dermal biopsy of the patient and three healthy gender-matched adult controls. Informed consent was obtained for the patient and her parents. Genomic DNA was extracted from peripheral blood (Qiagen, Hilden, Germany) following the manufacturer's instructions. Total RNA was extracted from lymphoblasts or fibroblasts using an RNeasy Plus Mini Kit (Qiagen), and retro-transcribed using the Transcriptor First Strand cDNA Synthesis kit (Roche Diagnostics, Mannheim, Germany).

Cytogenetic, Fluorescence In Situ Hybridization (FISH) analyses, array-CGH

Cytogenetic analysis of peripheral blood lymphocytes from the proband and both parents was performed using standard techniques. Array-CGH was carried out on genomic DNA using a whole genome oligonucleotide microarray platform (Human Genome CGH Microarray 244A Kit; Agilent Technologies, Santa Clara, California, USA) (see the supplement).

Mice tissue collection and RNA isolation

Thoc2 and *Ptk2* mRNA quantification was performed on tissues obtained from C57BL/6 mice at different ages from embryonic day 14 (E14) to two months postnatal (P60), including the day of birth (P0) (pools of three individuals per time point) (see the supplement).

In vitro transcription/translation

To obtain the chimeric *PTK2-THOC2* transcript, we amplified the patient's cDNA using a forward primer on exon 1 of the *PTK2* gene and a reverse primer on exon 12 of the *THOC2* gene. Transcription/translation was performed using TnT T7 Quick for PCR as described (Promega) (see the supplement).

Caenorhabditis elegans models, nematode strains, maintenance and gene silencing

Strains utilized in this work were N2:wild type Bristol, RB776: *kin-32*(ok166) I, and VC673: *thoc-2*(ok961) III/hT2[bli-4(e937) let-?(q782) qIs48] (I;III). We employed standard nematode culture conditions [9]. Strains were maintained at 20°C on Nematode Growth Media agar supplemented with *Escherichia coli* (OP50 or transformed HT115). Gene silencing was carried out through the RNA interference feeding technique as previously described [10] using bacteria transformed with L4440 empty vector as control, or L4440 containing dsRNA against *kin-32* (C30F8.4), or *thoc-2* (C16A3.8). Functional assays were performed as described in the supplement.

PTK2 expression induction

Patient's fibroblast cells (2×10^4) were plated on 24-well plates, cultured overnight, treated with 50 ng/ml of TNF-alpha (p.n. T6674, Sigma-Aldrich, St. Louis, MO, USA) for 6 h. Total RNA was collected using the Cells-to-Ct kit (Applied Biosystem) according to the manufacturer's protocols. Messanger RNA levels of *PTK2, PTK2-THOC2* fusion product and *THOC2* were determined by real-time RT-PCR as described in the supplement.

Rat hippocampal neurons and LC1 neuronal precursors culture and silencing

Primary cultures of rat hippocampal neurons were prepared from rat embryonic brains at E17.5 as previously described [9]. For morphological analysis in the first stages of development, $5\cdot10^5$ neurons were nucleofected with Amaxa Nucleofection Kit (Lonza, Cologne, Germany). Neurons were plated in MEM-Horse medium on poly-L-lysine pre-coated coverslips. After 4 hours, medium was changed in N2 medium and coverslips were flipped upside down. For morphological analysis $2\cdot10^5$ neurons were plated.

LC1 were plated (typically $2–3\cdot10^6$ cells into a T75 flask) on uncoated plastic in Neuromed N medium (Euroclone, Milan, Italy) supplemented with modified N2 [10] and 10 ng/ml of both EGF and FGF-2 (NS expansion medium). LC1 were detached with Accutase (Invitrogen), pelleted in PBS and then split into fresh plates. For transfection $8\cdot10^6$ cells were nucleofected with Amaxa Nucleofection Kit.

For transfection in hippocampal neurons and LC1 we used two efficient *Thoc2* siRNA constructs (Sh8137 and Sh2113, Ambion).

Rat hippocampal neurons grown on coverslips were fixed with 4% paraformaldehyde (PFA)/PBS for 10 minutes, then quenched with NH_4Cl 50 mM/PBS. Permeabilization was performed with 0.1% TritonX-100/PBS for 3 minutes and a 5% BSA/PBS saturation was left for 30 minutes over the coverslips. Following this step, primary antibodies were left for 1 hour and appropriate Alexa-conjugated secondary antibodies were used for 30 minutes followed by other three washings with PBS. Coverslips were mounted with Mowiol on cover glasses and analyzed with an inverted fluorescence microscope. All samples were examined using Apotome system (Zeiss).

The following primary antibodies were used: mouse monoclonal anti-SMI 312 (Covance), mouse monoclonal anti-alpha Tubulin (Sigma); counterstaining using Phalloidin (Sigma) for actin and DAPI (Sigma) for nuclei was used.

Further Materials and Methods are in the Supplement.

RESULTS

Clinical, neuroradiological, biochemical and genetic analyses

The patient was born after an uneventful pregnancy. No problems were reported at birth, in the perinatal period, and during the first year of life. Symptoms were noted at ~15 months when she started walking, and consisted of motor incoordination and unsteady gait. Brain magnetic resonance imaging (MRI) at 23 months revealed hypoplasia of the cerebellar hemispheres and vermis. MRI was repeated at ~ 6 yrs and corfirmed hypoplasia of the posterior fossa with low-set tentorium, not progressive over time. Both cerebellar hemispheres and vermis were hypoplastic with enlargement of the IV ventricle (Fig. 1A and supplemental Fig. 1).

At 8 yrs the patient underwent detailed clinical investigation: electrocardiogram was normal; mild dysmorphic features were noted: joint hypermobility, micrognathia leading to malocclusion, ogival palate, pointed chin, low-set and protruding ears, small hands (10^{th} centile) with tapering fingers and clinodactyly of the 4^{th} finger, hyperconvex toenails.

Neurological features included gait and limb ataxia, dysmetria, adiadochokinesia and diffuse hypothonia. The patient also presented with bradylalia, dysarthria, occasional dyslalia and pneumophonic coordination impairment. Babinski sign was present on the left foot only; osteotendinous reflexes were weak at the four limbs. Eye movements were normal and nystagmus was absent. Mild intellectual disability was present, with impaired visual and spatial orientation. Moreover, aggressive behavior and socially inappropriate and derogatory remarks (coprolalia) were reported. Biochemical blood analyses were normal. Serum alpha-fetoprotein was within normal range. Sialoglycoprotein deficits were ruled out by laboratory testing. Friedreich's ataxia was excluded by routine genetic testing.

Cytogenetic analysis

Chromosome analysis found a translocation involving chromosomes X and 8: 46,X,t(X;8)(q25;q24.3) (Fig. 1B). The normal karyotype of the parents and the segregation of polymorphic markers (Profiler Plus kit, Applied Biosystems) demonstrated that the translocation was *de novo*. FISH analysis with probes painting the X chromosome confirmed the translocation (data not shown), and a subtelomeric 8q probe (Vysis) proved that a small telomeric 8q region was translocated on the der(X) chromosome. Array-CGH analysis using a 244 K array (Agilent Technologies) did not reveal genomic deletion/duplication besides a few known copy number variants.

X-inactivation was completely skewed in the proband (see the supplement, fig. 1C), with the active allele inherited from the father.

Mapping and characterization of the breakpoint junctions

We mapped the breakpoint to a region of ~ 37 kb and defined the translocation between 8q24.3 and Xq25 by FISH (Fig. 1D and 1E; details in the supplement).

We used a set of forward and reverse primers to amplify the breakpoint junctions on the two derivatives. The two breakpoints were located in nonhomologous regions, involving repetitive elements: MER4/AluJ on chromosome 8 and SVA element on chromosome X (Supplement figure 2). A segment of 88 bp was lost on the X chromosome in the translocation.

The translocation interrupted the *PTK2* gene at 8q24.3 in the 5′-UTR between exons 1 and 2, ~30 kb from the transcription start site, whereas no known gene was interrupted at Xq25. However, the transcription start site of the closest gene, *THOC2*, lay only 2 kb downstream of the breakpoint (see scheme in Fig. 1E).

PTK2 and THOC2 gene expression analyses

We initially evaluated *PTK2* gene expression by mRNA and protein analysis. (i) We showed that the rs7460 SNP, heterozygous in the patient's genomic DNA, was expressed only from the paternal allele (Fig. 2A). Real-time PCR on total RNA from fibroblasts showed a half-dose of the *PTK2* gene in the patient (0.5 ± 0.05, mean ± S.D.) compared to normal controls (1.0 ± 0.1, mean ± S.D., $p < 0.001$) (Fig. 2B). Western blot confirmed protein reduction in the patient (0.7 ± 0.1, mean ± S.D.) vs. controls (1.0 ± 0.05, mean ± S.D.) (Fig. 2C).

THOC2 showed an apparent mRNA overexpression (patient = 2.8 ± 0.025, mean ± S.D., controls = 1 ± 0.06, $p < 0.001$) with a real-time PCR assay on exons 33–34 from patient's fibroblasts (Fig. 2D). However, using an assay on exons 1–2 of the *THOC2* gene revealed a transcript reduction to about half the dose of controls (patient= 0.5 ± 0.035, mean ± S.D.; controls = 1 ± 0.06, $p < 0.01$) (Fig. 2D) THOC2 protein levels were also significantly reduced (patient = 0.4 ± 0.1, mean ± S.D., controls = 1 ± 0.9, $p < 0.01$, two-tailed Student's t-test) (Fig. 2E).

To test the effect of the translocation on *THOC2* flanking genes, we measured the expression of *GRIA3* (patient= 0.97±0.04, controls= 1 ± 0.05, mean ± S.D.) and *XIAP* (patient 0.93 ± 0.10, controls 1 ± 0.08, mean ± S.D.) vs. *TBP* in the patient's fibroblasts. Expression of both genes was similar to controls.

We reasoned that even if the breakpoint on the der(X) lay outside the *THOC2* coding sequence, it could alter *THOC2* expression by transcriptional interference.

PTK2-THOC2 fusion sterile transcript

The above results suggested that two different mRNAs were produced from the der(X): a less abundant, corresponding to the wild type transcript, initiated at the *THOC2* transcription start site (TSS), and a more abundant, fusion transcript under the control of the *PTK2* promoter. The fusion transcript was confirmed by RT-PCR on RNA from the patient's fibroblasts, using a forward primer within *PTK2* exon 1, and a reverse primer in *THOC2* exon 2 (Fig. 3A). The sequence of the PCR product showed the skipping of *THOC2* exon 1,

likely because the first exon does not have an acceptor splice site (see scheme in Fig. 3A). The expected sterility of the fusion transcript was confirmed in vitro through a coupled transcription/translation assay: as shown in figure 3B, the 45.7 kDa protein produced in the control lane was absent in the transcribed and translated *PTK2-THOC2* construct (see also the supplement).

PTK2 promoter transcriptional interference on THOC2

To evaluate whether expression of the fusion transcript affected expression of the wild type *PTK2* allele, we treated the patient's fibroblasts with 50 ng/ml TNF-alpha for 6 hours, known to induce *PTK2* expression [11]. By real-time PCR, we measured expression of wild type *PTK2*, wild type *THOC2* (exons 1–2) and the sum of wild type *THOC2* and the fusion transcript (with an assay on *THOC2* exons 33–34). Under these conditions, wild type *PTK2* mRNA was significantly induced (untreated cells = 1 ± 0.032, mean ± S.D., treated cells = 1.5 ± 0.048, $p < 0.001$) (Fig. 3C). TNF-alpha also elicited a ~60% increase in expression of total *THOC2* mRNA (untreated cells 1 ± 0.037, mean ± S.D., treated cells 1.6 ± 0.084, $p<0.001$), but at the same time produced ~10% reduction of the wild type *THOC2* (untreated cells 1 ± 0.034, mean ± S.D., treated cells 0.9 ± 0.016, $p=0.0052$) (Fig. 3C).

Ptk2 and Thoc2 expression in mouse brain

To better interpret the results obtained in the patient's cells, we investigated *PTK2* and *THOC2* function in cellular and animal models.

We measured *Ptk2* and *Thoc2* mRNA expression in murine brain and cerebellum at different developmental stages (E14, P0, P60) (Fig. 4A, B). Expression of both genes seemed to increase from embryonic to adult life in the two tissues. It has been shown by *in situ* hybridization experiments, using an antisense probe, that *Thoc2* is highly expressed in brain, especially in the frontal cortex, and selectively expressed in the cerebellar region corresponding to the Purkinje cell layer (Fig. 4C, D Allen Institute for Brain Science. ©2009. http://mouse.brain-map.org, experiment 69444837).

Kin-32 and thoc-2 models in C. elegans

C. elegans has one *THOC2* homolog known as *thoc-2* or *tag-13*, and one *PTK2* homolog known as *kin-32*. *Kin-32* encodes, by alternative splicing, two isoforms of a focal adhesion kinase, orthologous to human *PTK2* and *PTK2B* [12]. Consistent with previous findings [12], we observed that *kin-32* knockout animals were viable, fertile and did not show anomalies in development, locomotion or chemosensory activity. On the other hand, *thoc-2* appears to be necessary for animal viability (www.wormbase.org). A strain containing a large, *thoc-2* homozygous, lethal deletion toward the C-terminus of the *thoc-2* gene (ok961) is therefore maintained as a balanced heterozygote with a *bli-4*- and GFP-marked translocation. *C. elegans thoc-2* knockouts (25%) were slow-growing, became sterile adults with vulve defects (www.wormbase.org) and died prematurely (*our unpublished observation*).

Animals *thoc-2*$^{+/+}$ (25%) were not viable due to segregation with the homozygous lethal *bli-4* balancer; *thoc-2*$^{+/-}$ were instead wild-type-looking animals, with normal fertility and

slightly retarded development. Further experiments were therefore performed on *thoc-2*$^{+/-}$ and *thoc-2*$^{-/-}$ animals.

Animals *thoc-2*$^{-/-}$ were almost completely immobile, or moved slowly and for a short time upon touching. Locomotion was also statistically reduced in heterozygotes (Fig. 5A). On the other hand, mechanosensory neurons were not affected in either genotypes, as shown by a normal response to head and tail touch (data not shown). The chemotaxis index, tested in a mixed population of *thoc-2* knockouts and heterozygotes, was significantly reduced for different attractants/repulsive chemicals, proving a defect in specific sensory neurons (Fig. 5B).

Thoc2 knockdown in mouse LC-1 cells and in rat hippocampal cells

The anatomical and functional abnormalities detected in the patient suggested that a reduced dosage of *THOC2* could determine specific abnormalities in the proliferation, differentiation and/or survival of neuronal precursor cells or in the survival of differentiated neurons. To address these possibilities, we conducted knockdown studies in rodent cells transfected with shRNA constructs capable of reducing the *Thoc2* ortholog expression by approximately 70% in HeLa cells (data not shown). To analyze the possible effects of *Thoc2* knockdown on the expansion of neuronal precursors we used mouse LC-1 cells, which are positive for the neuronal progenitor marker nestin and rapidly proliferate in presence of FGF2 and EGF, but differentiate with high efficiency into neurons and astrocytes when cultured without growth factors [13]. On the other hand, to address the role of *Thoc2* in neuronal differentiation, we resorted to rat hippocampal neurons in primary culture [14]. These cells were transfected with shRNA constructs before plating and allowed to differentiate for ~72 hours. In both systems, *Thoc2* silencing did not increase significantly the number of apoptotic cells (data not shown), thus excluding that *Thoc2* knockdown affected neuronal cell viability. On the contrary, *Thoc2*-depleted LC-1 cells displayed a significantly increased proliferation rate, as determined by the MTT assay (Fig. 6A). In differentiating primary hippocampal neurons, the knockdown of *Thoc2* produced a significant increase in the length of neuronal processes (Fig. 6B–C), without affecting the timing of transitions between the first differentiation stages (data not shown).

DISCUSSION

Chromosomal rearrangements have been instrumental in identifying disease-causing genes located across or near the breakpoints [15, 16]. Here we describe a *de novo* reciprocal translocation between Xq25-ter and 8q24.3-ter, associated with psychomotor retardation and congenital cerebellar hypoplasia, likely caused by altered expression of two genes, *PTK2* at 8q24.3 and *THOC2* at Xq25. The 8q24.3 breakpoint occurred within the *PTK2* gene. As expected, the mRNA and PTK2 protein levels were reduced to 50% in the patient's fibroblasts, compared to healthy controls. The absence of mutation in the transcript expressed by the second *PTK2* allele does not support the hypothesis of a recessive phenotype. *PTK2* encodes a cytosolic protein tyrosine kinase involved in focal adhesion formation [17]. Its activity elicits intracellular signal transduction pathways that stimulate the turnover of cell contacts with the extracellular matrix, promoting cell migration. PTK2

has been implicated in central nervous system development and myelination, and synaptic plasticity in the mouse hippocampus [18, 19, 20].

Although we cannot exclude that *PTK2* haploinsufficiency played some role in our patient's phenotype, it is worth noting that: (a) micro- and macro-deletions (~120 kb to 6.9 Mb) containing *PTK2* have been reported in at least two healthy parents of children with cognitive impairment, with or without malformations (ref: #255112 Decipher Database; #11255_85 Rome, Italian Database of Copy Number Variants, http://dbcnv.oasi.en.it); (b) *Ptk2* homozygous knockout is lethal in mice, whereas haploinsufficiency does not result in a pathological phenotype [21]. Purkinje cells from homozygous conditional knockout mice show a normal phenotype [22]; (c) *kin-32* (*PTK2* ortholog) silencing in *C. elegans* did not affect viability, development, fertility, locomotion and chemosensory activity.

The Xq25 translocation created a fusion product which maintained both the *PTK2* and *THOC2* promoters. We demonstrated that the transcription of the *PTK2 – THOC2* fusion gene, under the *PTK2* promoter, downregulates the level of the wild type *THOC2* mRNA and protein.

Such a phenomenon, known as transcriptional interference [23], is responsible of a variety of human diseases, e.g., alpha-thalassemia (a gain-of-function, regulatory single-nucleotide polymorphism creates a new promoter-like element that interferes with normal activation of all downstream alpha-like globin genes [24]); Lynch syndrome: *TACSTD1* – a gene upstream to the Mismatch repair *MSH2* gene, transcribed in the same direction – not rarely shows deletions spanning the last exon, including the polyA signal. The RNA polymerase proceeds, interfering with the transcription of the downstream *MSH2* promoter, and gives rise to *TACSTD1/MSH2* fusion transcripts [25].

THOC2 product is a subunit of a multiprotein complex called the THO complex, which is conserved from yeast to humans [26]. THO interacts physically and functionally with the mRNA export factors Yra1 and Sub2 forming the TREX (TRanscription-EXport) complex.

It has been shown that TREX plays a role in mRNA transport from the nucleus to cytoplasm and distinct pathophysiological states are correlated with defective mRNA export mechanisms [27]. *Thoc5* deletion in mice causes death in the first two weeks after birth, similar to *Thoc1* deletion. *Thoc5* conditional knockout mouse developes acute leukocytopenia and anemia, suggesting that the TREX complex has a key role not only in early embryogenesis, but also in differentiation, as previously reported with *Thoc1* knockout [28, 29]. Other mRNA export genes have been linked to human diseases, such as the fragile X mental retardation protein, FMRP, that regulates mRNA metabolism and translation of key molecules involved in receptor signalling and spine morphology [30].

THOC2 is expressed in murine brain, and its pattern in the cerebellum is compatible with Purkinje cells distribution, consistent with our patient's clinic-pathological phenotype. *PTK2* is also expressed in brain, but with a more diffuse pattern [22]. In the cerebellum, the generation of the different categories of neurons is accomplished through well-defined space and time constraints, regulated by signals which are only partially known [31]: downregulation of *THOC2*, possibly combined with *PTK2* haploinsufficiency, may lead to

aberrant timing of axonal sprouting or altered proliferation of specific neuronal populations, thus determining the cerebellar hypoplasia/cognitive impairment found in our patient.

Indeed, using fibroblasts from our patient, we demonstrated that when the *PTK2* gene was upregulated by TNF-alpha, the fusion transcript was overexpressed, whereas wild type *THOC2* gene was further repressed. We suggest that *THOC2* downregulation by transcriptional interference is a hypomorphic mutation and its expression may be further reduced in tissues where the ratio *PTK2/THOC2* favors the former.

The possible role of *THOC2* in the pathogenesis of our patient's phenotype was supported by our findings in three cellular/animal models: (i) *thoc-2* gene knockout in *C.elegans* were almost completely immobile and *thoc-2*$^{+/-}$ had impaired locomotion activity. The function of sensory neurons (AWA, AWB, AWC, ASE) was significantly impaired even in a mixed population of heterozygotes and *thoc2* knockouts. (ii) In LC1 mouse neuronal precursors, downregulated *Thoc2* (~30% of the wild type) led to a significant increase in the proliferation, and (iii) in rat hippocampal primary neurons an increased length of neurites.

Overall, these data prove a neuronal defect driven by *THOC2* suppression and suggest that *THOC2* is a dosage-sensitive gene. Thus, *THOC2* may represent a further member of nuclear mRNA export factors, whose inappropriate interaction, expression pattern and possibly mRNA-binding specificity are expected to produce a variety of congenital syndromes, associated with brain diseases.

In conclusion, we describe a female with a cerebellar hypoplasia-psychomotor delay syndrome in which a chromosomal translocation alters the expression of two genes, *PTK2* and *THOC2*, involved in central nervous system. Our data and that of the literature suggest that the phenotype in our patient is due to the decreased expression of *THOC2*, or to a combined effect of *THOC2/PTK2* reduction, although no definitive evidence exists in support of one of these two hypotheses.

Supplementary Material

Refer to Web version on PubMed Central for supplementary material.

Acknowledgments

We are gratefully indebted to the family who participated in this study. This work was supported by, the VERUM foundation, the French Association Connaitre les Syndromes Cérébelleux, the National Ataxia Foundation, the "Associazione E.E. Rulfo per la Genetica Medica", and A.I.S.A. Piemonte. NV is recipient of "My First Airc Grant" (MFAG11509). The funding organizations had no role in study design, data collection and analysis, decision to publish, or preparation of the manuscript. We thank the clinicians who referred their patients, the technical assistance of Dr. P. Pappi (Medical Genetics Unit, A.O. Città della Salute e della Scienza, Turin, Italy), Drs. E. Ferrero and Nicola Migone (University of Turin) for her advice and critical reading of the manuscript, and all members of the DNA and Cell bank team of the Centre de Recherche de l'Institut du Cerveau et de la Moelle épinière (Paris, France). LC1 neural stem cells were a kind gift from Luciano Conti (Department of Pharmacological Science, University of Milan, Milan, Italy).

References

1. Steinlin M. Non-progressive congenital ataxias. Brain Dev. 1998; 20(4):199–208. [PubMed: 9661964]

2. Manto MU, Jissendi P. Cerebellum: links between development, developmental disorders and motor learning. Front Neuroanat. 2012; 6:1. [PubMed: 22291620]
3. Courchesne E, Townsend J, Akshoomoff NA, Saitoh O, Yeung-Courchesne R, Lincoln AJ, James HE, Haas RH, Schreibman L, Lau L. Impairment in shifting attention in autistic and cerebellar patients. Behav Neurosci. 1994; 108(5):848–65. [PubMed: 7826509]
4. Zanni G, Bertini ES. X-linked disorders with cerebellar dysgenesis. Orphanet J Rare Dis. 2011; 6:24. [PubMed: 21569638]
5. Zanni G, Saillour Y, Nagara M, Billuart P, Castelnau L, Moraine C, Faivre L, Bertini E, Durr A, Guichet A, Rodriguez D, des Portes V, Beldjord C, Chelly J. Oligophrenin 1 mutations frequently cause X-linked mental retardation with cerebellar hypoplasia. Neurology. 2005; 65(9):1364–9. [PubMed: 16221952]
6. Illarioshkin SN, Tanaka H, Markova ED, Nikolskaya NN, Ivanova-Smolenskaya IA, Tsuji S. X-linked nonprogressive congenital cerebellar hypoplasia: clinical description and mapping to chromosome Xq. Ann Neurol. 1996; 40(1):75–83. [PubMed: 8687195]
7. Bertini E, des Portes V, Zanni G, Santorelli F, Dionisi-Vici C, Vicari S, Fariello G, Chelly J. X-linked congenital ataxia: a clinical and genetic study. Am J Med Genet. 2000; 92(1):53–6. [PubMed: 10797423]
8. Zanni G, Bertini E, Bellcross C, Nedelec B, Froyen G, Neuhauser G, Opitz JM, Chelly J. X-linked congenital ataxia: a new locus maps to Xq25-q27. 1. Am J Med Genet A. 2008; 146A(5):593–600. [PubMed: 18241076]
9. Stiernagle T. Maintenance of C. elegans. WormBook. 2006:1–11. [PubMed: 18050451]
10. Ventura N, Rea SL, Schiavi A, Torgovnick A, Testi R, Johnson TE. p53/CEP-1 increases or decreases lifespan, depending on level of mitochondrial bioenergetic stress. Aging Cell. 2009; 8(4):380–93. [PubMed: 19416129]
11. Kurenova E, Xu LH, Yang X, Baldwin AS Jr, Craven RJ, Hanks SK, Liu ZG, Cance WG. Focal adhesion kinase suppresses apoptosis by binding to the death domain of receptor-interacting protein. Mol Cell Biol. 2004; 24(10):4361–71. [PubMed: 15121855]
12. Cram EJ, Fontanez KM, Schwarzbauer JE. Functional characterization of KIN-32, the Caenorhabditis elegans homolog of focal adhesion kinase. Dev Dyn. 2008; 237(3):837–46. [PubMed: 18297732]
13. Conti L, Pollard SM, Gorba T, Reitano E, Toselli M, Biella G, Sun Y, Sanzone S, Ying QL, Cattaneo E, Smith A. Niche-independent symmetrical self-renewal of a mammalian tissue stem cell. PLoS Biol. 2005; 3(9):e283. [PubMed: 16086633]
14. Banker G, Goslin K. Developments in neuronal cell culture. Nature. 1988; 336(6195):185–6. [PubMed: 3185736]
15. Billuart P, Bienvenu T, Ronce N, des Portes V, Vinet MC, Zemni R, Carrie A, Beldjord C, Kahn A, Moraine C, Chelly J. Oligophrenin 1 encodes a rho-GAP protein involved in X-linked mental retardation. Pathol Biol (Paris). 1998; 46(9):678. [PubMed: 9885813]
16. Najm J, Horn D, Wimplinger I, Golden JA, Chizhikov VV, Sudi J, Christian SL, Ullmann R, Kuechler A, Haas CA, Flubacher A, Charnas LR, Uyanik G, Frank U, Klopocki E, Dobyns WB, Kutsche K. Mutations of CASK cause an X-linked brain malformation phenotype with microcephaly and hypoplasia of the brainstem and cerebellum. Nat Genet. 2008; 40(9):1065–7. [PubMed: 19165920]
17. Andre E, Becker-Andre M. Expression of an N-terminally truncated form of human focal adhesion kinase in brain. Biochem Biophys Res Commun. 1993; 190(1):140–7. [PubMed: 8422239]
18. Beggs HE, Schahin-Reed D, Zang K, Goebbels S, Nave KA, Gorski J, Jones KR, Sretavan D, Reichardt LF. FAK deficiency in cells contributing to the basal lamina results in cortical abnormalities resembling congenital muscular dystrophies. Neuron. 2003; 40(3):501–14. [PubMed: 14642275]
19. Rico B, Beggs HE, Schahin-Reed D, Kimes N, Schmidt A, Reichardt LF. Control of axonal branching and synapse formation by focal adhesion kinase. Nat Neurosci. 2004; 7(10):1059–69. [PubMed: 15378065]

20. Monje FJ, Kim EJ, Pollak DD, Cabatic M, Li L, Baston A, Lubec G. Focal adhesion kinase regulates neuronal growth, synaptic plasticity and hippocampus-dependent spatial learning and memory. Neurosignals. 2012; 20(1):1–14. [PubMed: 21952616]
21. Ilic D, Furuta Y, Kanazawa S, Takeda N, Sobue K, Nakatsuji N, Nomura S, Fujimoto J, Okada M, Yamamoto T. Reduced cell motility and enhanced focal adhesion contact formation in cells from FAK-deficient mice. Nature. 1995; 377(6549):539–44. [PubMed: 7566154]
22. Watanabe F, Miyazaki T, Takeuchi T, Fukaya M, Nomura T, Noguchi S, Mori H, Sakimura K, Watanabe M, Mishina M. Effects of FAK ablation on cerebellar foliation, Bergmann glia positioning and climbing fiber territory on Purkinje cells. Eur J Neurosci. 2008; 27(4):836–54. [PubMed: 18279360]
23. Palmer AC, Egan JB, Shearwin KE. Transcriptional interference by RNA polymerase pausing and dislodgement of transcription factors. Transcription. 2011; 2(1):9–14. [PubMed: 21326903]
24. De Gobbi M, Viprakasit V, Hughes JR, Fisher C, Buckle VJ, Ayyub H, Gibbons RJ, Vernimmen D, Yoshinaga Y, de Jong P, Cheng JF, Rubin EM, Wood WG, Bowden D, Higgs DR. A regulatory SNP causes a human genetic disease by creating a new transcriptional promoter. Science. 2006; 312(5777):1215–7. [PubMed: 16728641]
25. Kovacs ME, Papp J, Szentirmay Z, Otto S, Olah E. Deletions removing the last exon of TACSTD1 constitute a distinct class of mutations predisposing to Lynch syndrome. Hum Mutat. 2009; 30(2): 197–203. [PubMed: 19177550]
26. Reed R, Cheng H. TREX, SR proteins and export of mRNA. Curr Opin Cell Biol. 2005; 17(3): 269–73. [PubMed: 15901496]
27. Rondon AG, Jimeno S, Aguilera A. The interface between transcription and mRNP export: from THO to THSC/TREX-2. Biochim Biophys Acta. 2010; 1799(8):533–8. [PubMed: 20601280]
28. Mancini A, Niemann-Seyde SC, Pankow R, El Bounkari O, Klebba-Farber S, Koch A, Jaworska E, Spooncer E, Gruber AD, Whetton AD, Tamura T. THOC5/FMIP, an mRNA export TREX complex protein, is essential for hematopoietic primitive cell survival in vivo. BMC Biol. 2010; 8:1. [PubMed: 20051105]
29. Wang X, Chinnam M, Wang J, Wang Y, Zhang X, Marcon E, Moens P, Goodrich DW. Thoc1 deficiency compromises gene expression necessary for normal testis development in the mouse. Mol Cell Biol. 2009; 29(10):2794–803. [PubMed: 19307311]
30. Bagni C, Tassone F, Neri G, Hagerman R. Fragile X syndrome: causes, diagnosis, mechanisms, and therapeutics. J Clin Invest. 2012; 122(12):4314–22. [PubMed: 23202739]
31. Carletti B, Williams IM, Leto K, Nakajima K, Magrassi L, Rossi F. Time constraints and positional cues in the developing cerebellum regulate Purkinje cell placement in the cortical architecture. Dev Biol. 2008; 317(1):147–60. [PubMed: 18384765]

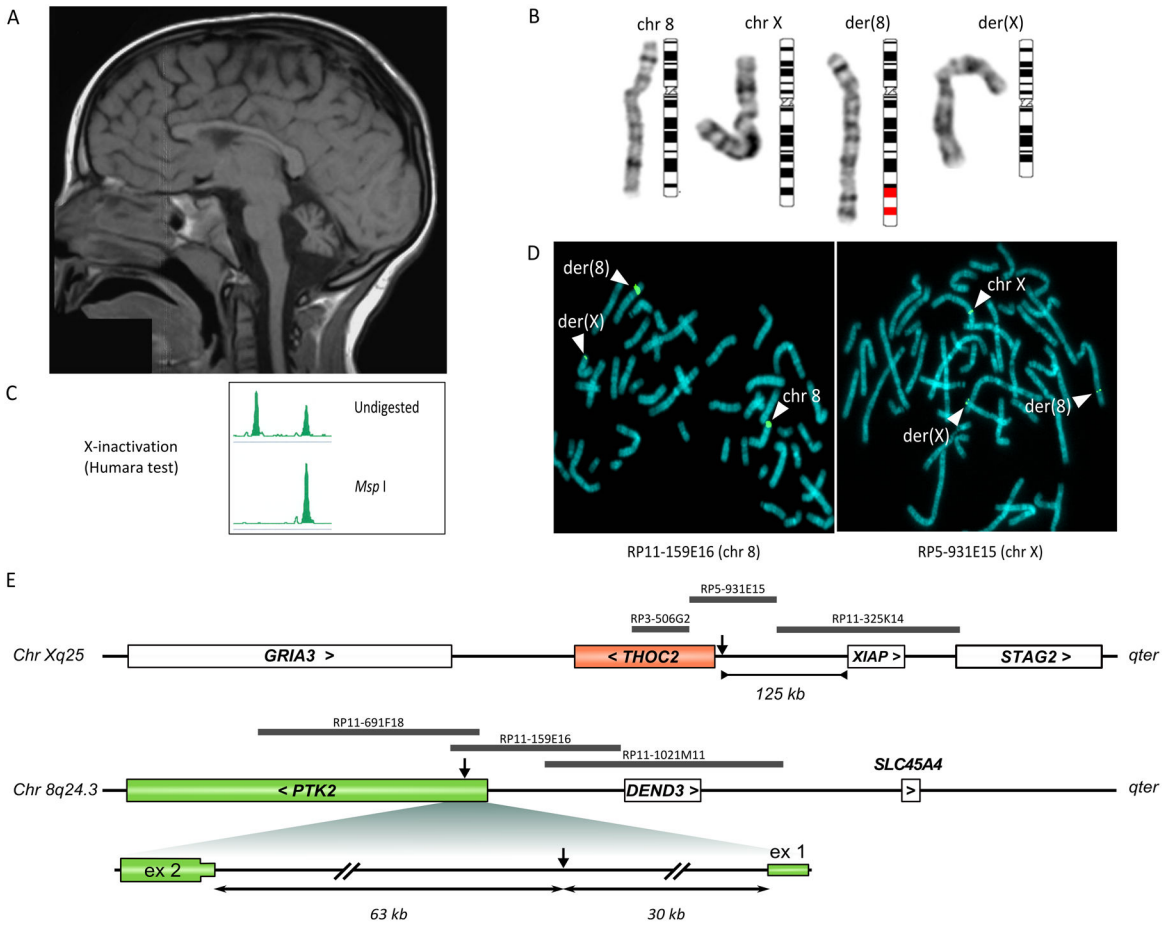

Figure 1. Patient's MRI, karyotype, X-inactivation and FISH analysis

(A) T1-weighted magnetic resonance imaging of the patient at 6 yrs showed hypoplasia of the cerebellar vermis, with enlargement of the IV ventricle and cisterna magna (see also supplement figure 1). (B) A translocation involving chromosome bands Xq25 and 8q24 was initially identified in the patient by standard karyotype. (C) X-inactivation analysis in the patient using the "humara test" showed a completely skewed pattern. (D) FISH analysis using two representative probes, one for chromosome 8 (RP11-159E16) and one for chromosome X (RP5-931E15) revealed the two derivatives and allowed definition of the breakpoint region. (E) Schematic representation of the Xq25 and 8q24.3 regions involved in the translocation. Genes are indicated as white or coloured boxes. The gene name is followed by a symbol indicating transcription direction. FISH probes used to define the breakpoint interval are indicated as grey bars. The breakpoint within the *PTK2* gene is enlarged.

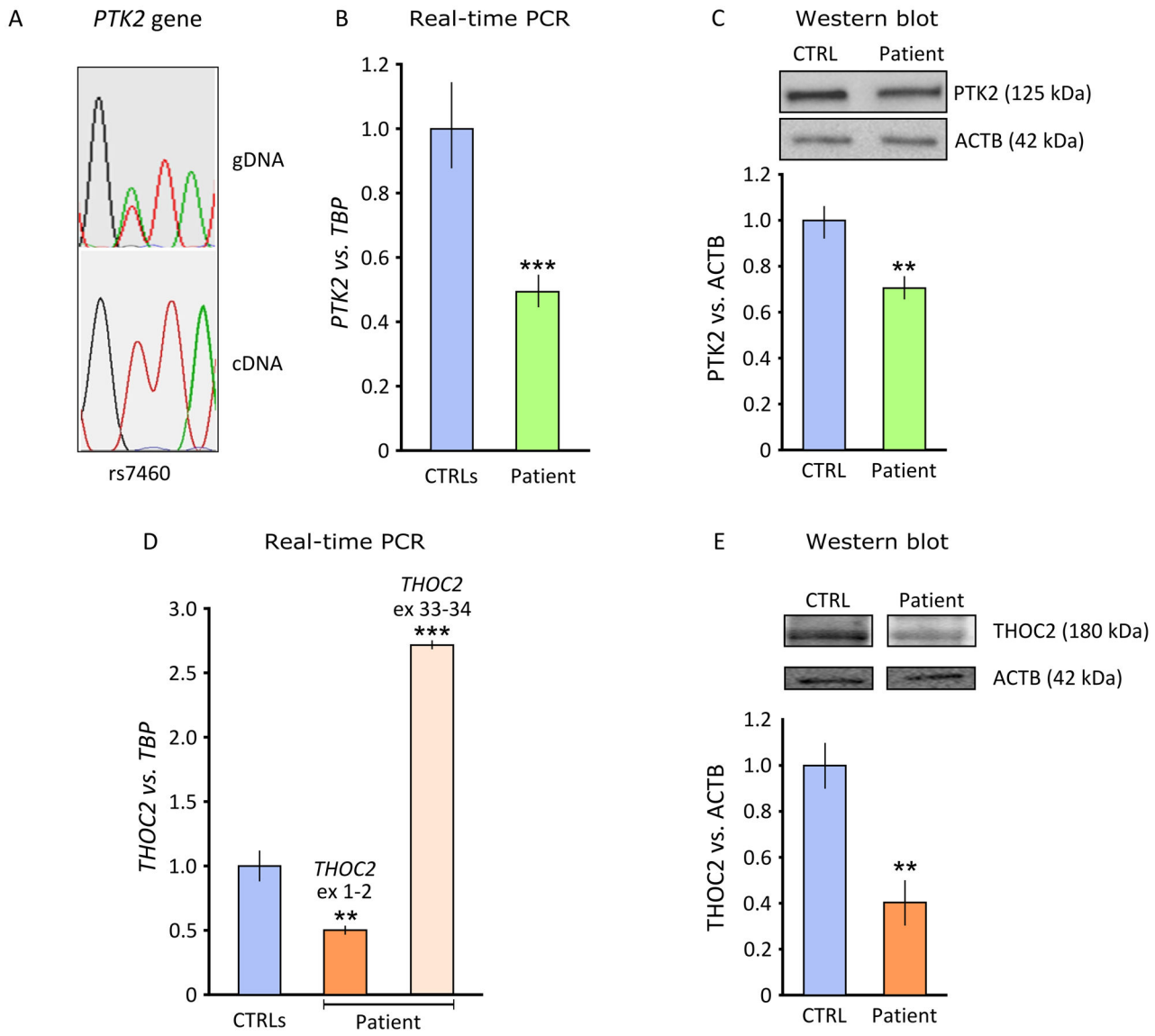

Figure 2. Expression analysis of *PTK2* and *THOC2* genes in patient's cells

(A) Sequence analysis of patient's genomic DNA (gDNA) and cDNA at SNP rs7460 in exon 32 of the *PTK2* gene. Only the maternal "T" allele was expressed. (B) Real-time PCR on the patient's cDNA extracted from fibroblasts showed a reduction of the *PTK2* gene measured vs. *TBP* reference (***p<0.001). (C) Reduction was confirmed at protein level vs. beta actin (ACTB) (**p<0.01). (D) Expression analysis of the *THOC2* gene (assay on exons 1–2) showed a ~50% reduction (reference gene *TBP*). However, using an assay on the 3′-end of the gene, *THOC2* transcript is apparently increased (***p<0.001, assay on exons 33–34). (E) *THOC2* reduction was confirmed at protein level vs. beta actin (ACTB) (**p<0.01). Statistic analysis was performed using a two-tailed Student's t-test.

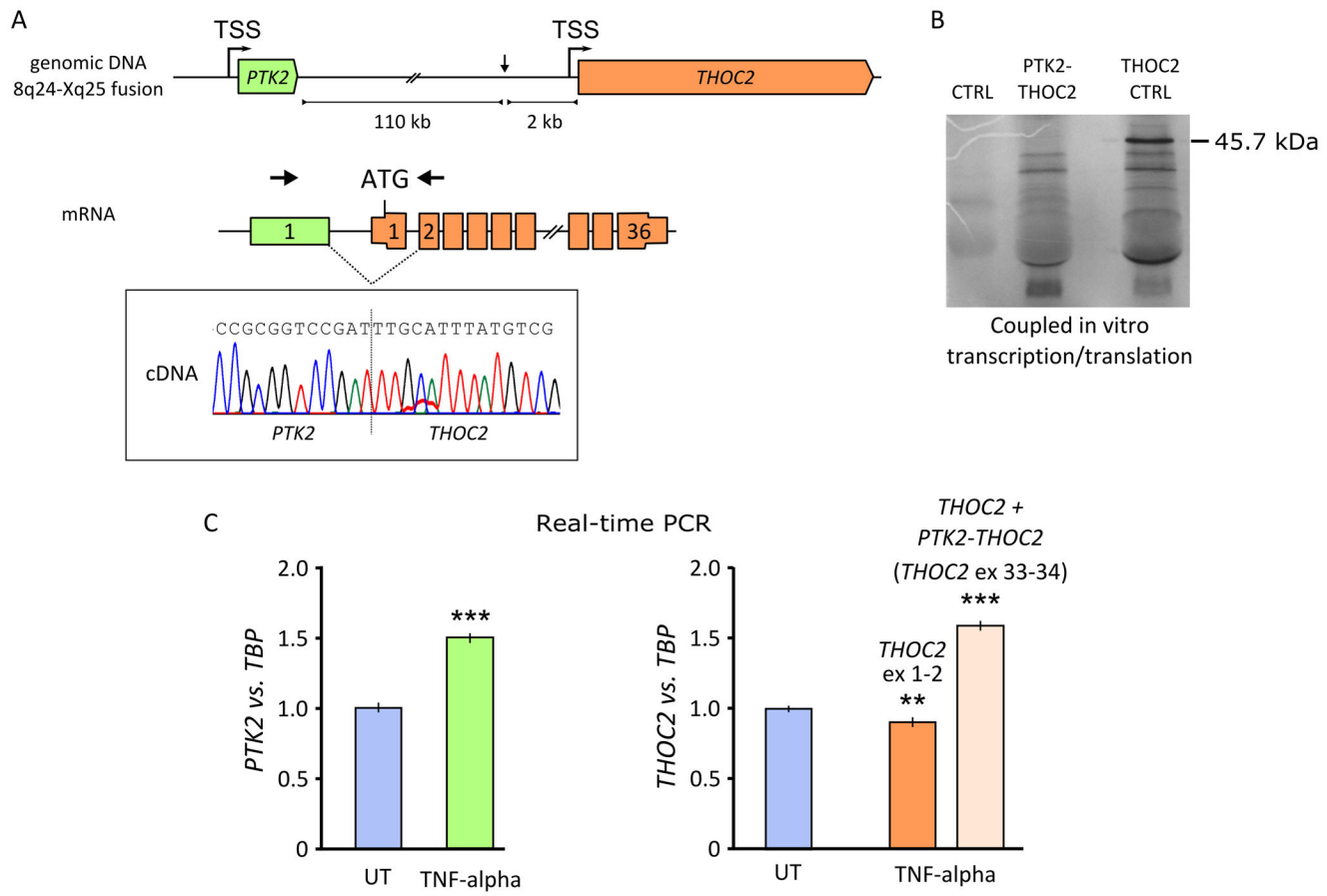

Figure 3. *PTK2-THOC2* fusion transcript

(A) The translocation juxtaposed *PTK2* to *THOC2* in the same transcriptional orientation (arrows). The *PTK2* promoter transcribed the *THOC2* gene; splicing generated a fusion transcript that lacks *THOC2* exon 1 (arrows indicate primers position to amplify the fusion transcript). (B) Coupled in vitro transcription/translation of a plasmid containing the fusion transcript (*PTK2* exon 1-*THOC2* exon 1–12) and a control insert (*THOC2* exons 1–12) showed that no internal translation start site is used by the fusion transcript, which did not code. The expected weight of the THOC2 wt protein coded by exons 1 to 12 is 45.7 kDa. (C) Six hours treatment with 50 ng/ml of TNF-alpha induced *PTK2* mRNA expression in fibroblasts from the patient. Real-time PCR showed an increase of the *PTK2* (untreated cells 1 ± 0.032, mean ± S.D., treated cells 1.5 ± 0.048, ***p<0.001) and *PTK2-THOC2* fusion product (assay on exons 33–34) expression (untreated cells 1 ± 0.037, mean ± S.D., treated cells 1.6 ± 0.084, ***p<0.001) relative to *TBP*. A reduction of *THOC2* expression vs. *TBP* was shown by real-time PCR assay on exon 1–2 (untreated cells 1 ± 0.034, mean ± S.D., treated cells 0.9 ± 0.016, **p=0.0052). Statistic analysis was performed using a two-tailed Student's t-test. UT: untreated cells; TSS: Transcription Start Site.

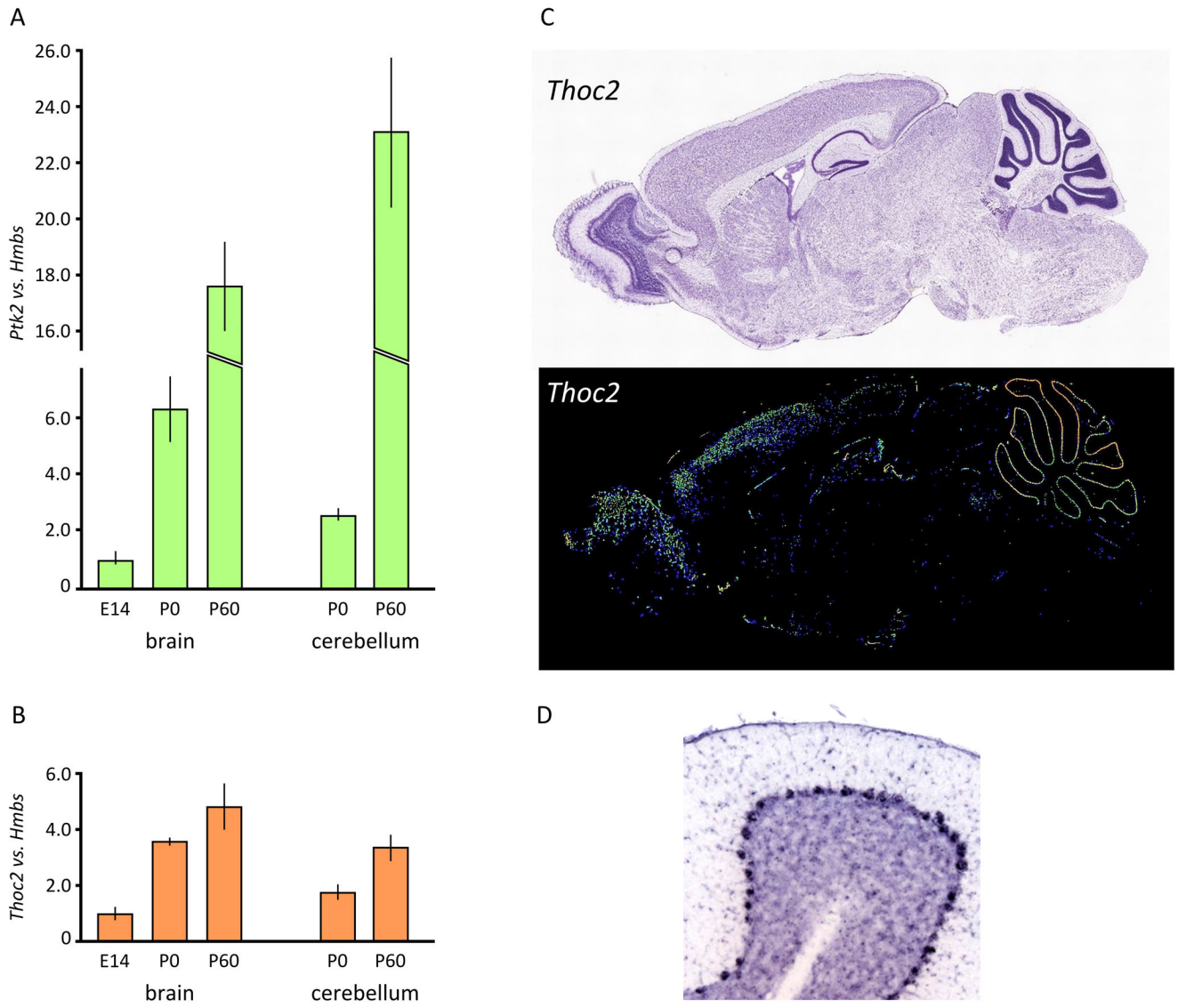

Figure 4. Expression analysis of *Ptk2* and *Thoc2* in mouse brain

(A)–(B) Expression analysis of *Ptk2 and Thoc2* genes vs. *Hmbs* in murine brain or cerebellar lysates by real-time RT-PCR, at different developmental stages (E14, P0, P60). *Ptk2* and *Thoc2* increased their expression during mouse development (brain from E14 to P60; cerebellum from P0 to P60). (C) *Thoc2 in situ* hybridization (above Nissl, and below *Thoc2 In Situ* Hybridisation (ISH) expression highlighted) in adult mouse brain shows that the gene is highly expressed, with a prevalence in frontal cortex and cerebellum. In this last tissue, the pattern is compatible with Purkinje neurons (see enlargement in panel D)(Allen Institute for Brain Science. ©2009. Available from: http://mouse.brain-map.org).

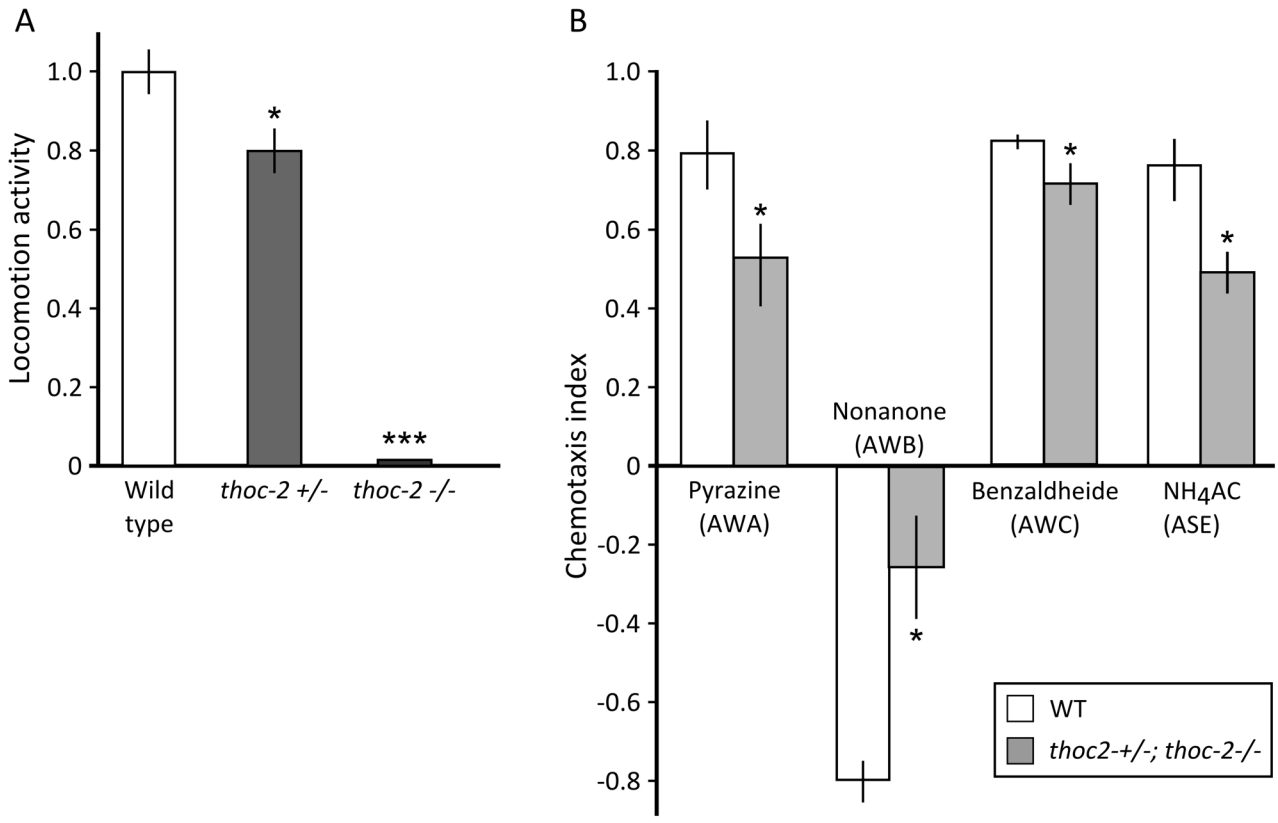

Figure 5. Characterization of *C. elegans* neuronal features

(A) Locomotion activity (body bends) in wild type, *thoc-2*$^{+/-}$ and *thoc-2*$^{-/-}$ one day-old adult animals, and (B) sensory function (chemotaxis index). The functionality of a specific subset of animal sensory neurons (AWA, AWB, AWC, ASE) was assessed by quantifying their attraction or repulsion to specific chemicals (respectively: pyrazine, nonanone, benzaldheide, NH_4Acetate). Bars represent mean of data coming from two to four independent experiments, each time carried in duplicate from two independent operators; error bars represent standard error of the mean (SEM); *p<0.05, ***p<0.001, two-tailed, unpaired Student's t-test.

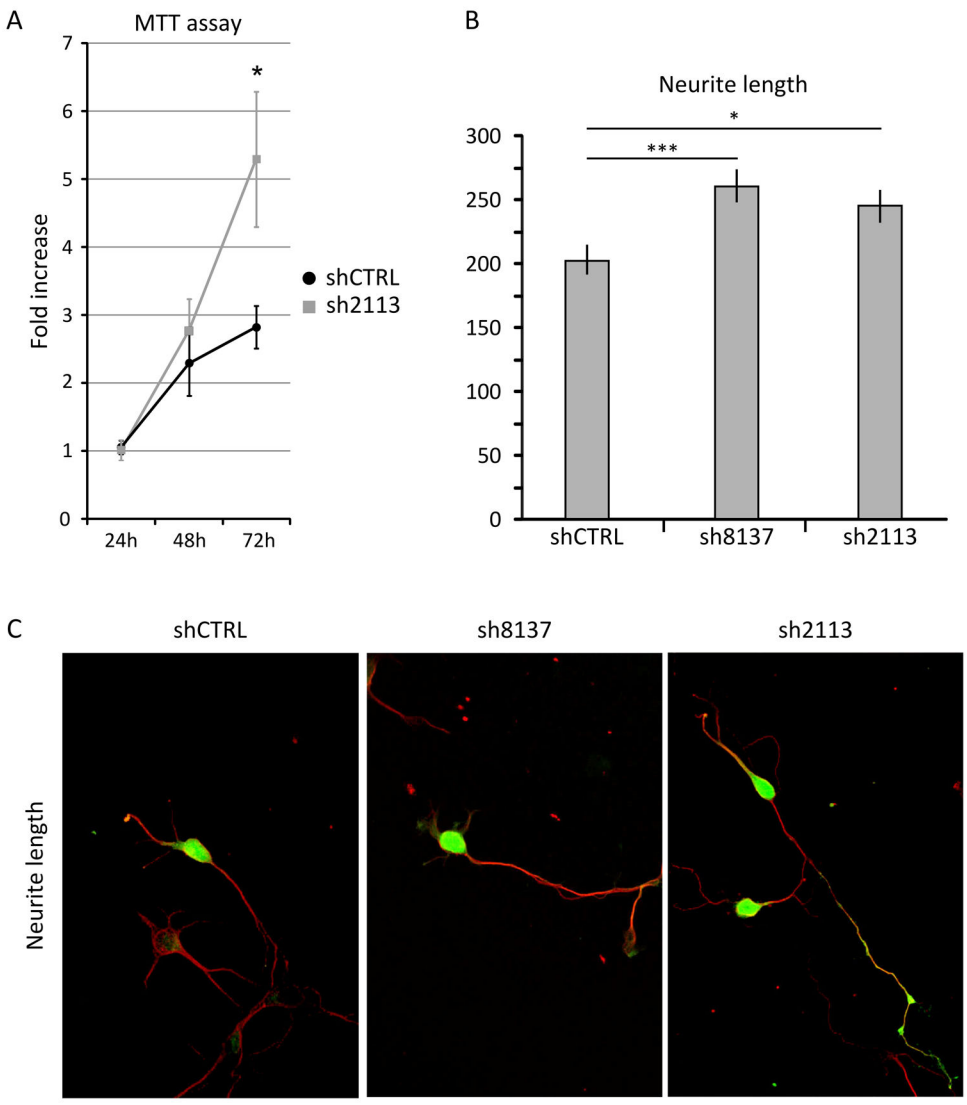

Figure 6. *Thoc2* knockdown in LC1 neural precursor cells and rat hippocampal neurons

(A) *Thoc2* knockdown stimulated the proliferation of LC1 neural precursor cells in culture. Neural precursor LC1 were electroporated with a scramble shRNA (shCTRL) or with specific shRNA expressing plasmid (sh2113) before plating, and allowed to proliferate in culture for 24h, 48h and 72h. The proliferation rate was measured using the MTT assay. *Thoc2* knockdown neurons grew faster than control cells ($p<0.05$, two-tailed, paired Student's t-test). (B–C) Primary rat hippocampal neurons were electroporated before plating with control (shCTRL) or specific shRNA-expressing plasmids (sh8137, sh2113) and allowed to differentiate for three days. The knockdown of *Thoc2* gene stimulated neurite outgrowth (*$p<0.05$, **$p<0.01$, ***$p<0.001$, two-tailed, unpaired Student's t-test). Green signal in the transfected cells is GFP and red signal is the staining for Alpha-Tubulin (C).